

Supplementary Information

Quinolines by Three-Component Reaction: Synthesis and Photophysical Studies

Eric S. Sales,^a Juliana M. F. M. Schneider,^a Marcos J. L. Santos,^a Adailton J. Bortoluzzi,^b
Daniel R. Cardoso,^c Willy G. Santos*^c and Aloir A. Merlo*^a

^aInstituto de Química, Universidade Federal do Rio Grande do Sul (UFRGS),
90040-060 Porto Alegre-RS, Brazil

^bDepartamento de Química, Universidade Federal de Santa Catarina(UFSC),
88040-900 Florianópolis-SC, Brazil

^cChemistry Institute of São Carlos, Universidade de São Paulo (USP),
13566-590 São Carlos-SP, Brazil

Experimental data

Data for 4-*n*-octyloxybenzaldehyde (**2a**). ¹H NMR (300 MHz, CDCl₃) δ (ppm) 9.87 (s, 1H, CHO), 7.83 (d, *J* 8.4 Hz, 2H, Ar-H), 6.99 (d, *J* 8.4 Hz, 2H, Ar-H), 4.05 (t, *J* 7.0 Hz, 2H, CH₂O), 1.78 (m, 2H, CH₂CH₂O), 1.53-1.22 (m, 10H, (CH₂)₈), 0.89 (t, *J* 7.0 Hz, 3H, CH₃).

Data for 4-*n*-nonyloxyaniline (**4a**). Yield 90%; white solid; m.p. 42 °C; ¹H NMR (300 MHz, CDCl₃) δ (ppm) 7.17 (d, *J* 8.5 Hz, 2H, Ar-H), 6.80 (d, *J* 8.8 Hz, 2H, Ar-H), 6.08 (broad, 2H, NH₂), 3.89 (t, *J* 6.5 Hz, 2H, CH₂O), 1.77 (m, 2H, CH₂CH₂O), 1.45-1.39 (m, 12H, (CH₂)₁₀), 0.89 (t, *J* 7.0 Hz, 3H, CH₃).

Data for 2-*n*-octyloxyaniline (**4b**). Yield 93%; white wax; ¹H NMR (300 MHz, CDCl₃) δ (ppm) 6.83 (m, 4H, Ar-H), 4.26 (broad, 2H, NH₂), 4.01 (t, *J* 6.8 Hz, 2H, CH₂O), 1.85 (m, 2H, CH₂CH₂O), 1.54-1.38 (m, 10H, (CH₂)₈), 0.90 (q, *J* 7 Hz, 3H, CH₃).

4-methoxyaniline (*p*-anisidine) (**4c**) was purchased from Aldrich Co.

Data for 1-ethynyl-4-heptyloxybenzene (**7a**). Yield 70%; colorless oil; ¹H NMR (300MHz, CDCl₃) δ (ppm) 7.26 (d, *J* 8.5 Hz, 2H, Ar-H), 6.67 (d, *J* 8.4 Hz, 2H, Ar-H),

3.77 (t, *J* 6.0 Hz, 2H, CH₂O), 2.85 (s, 1H, CCH), 1.63 (m, 2H, CH₂CH₂O), 1.30-1.20 (m, 8H, (CH₂)₆), 0.78 (t, *J* 6.5 Hz, 3H, CH₃); ¹³C NMR (75 MHz, CDCl₃) δ (ppm) 160.13, 134.09, 115.00, 114.59, 84.36, 76.30, 68.58, 32.42, 29.83, 29.71, 26.61, 23.25, 14.69.

Data for 1-ethynyl-4-octyloxybenzene (**7b**). Yield 85%; colorless oil; ¹H NMR (300 MHz, CDCl₃) δ (ppm) 7.45 (d, *J* 8.5 Hz, 2H, Ar-H), 6.85 (d, *J* 8.4 Hz, 2H, Ar-H), 3.94 (t, *J* 6.0 Hz, 2H, CH₂O), 3.02 (s, 1H, CCH), 1.80 (m, 2H, CH₂CH₂O), 1.50-1.32 (m, 8H, (CH₂)₆), 0.94 (t, *J* 6.5 Hz, 3H, CH₃); ¹³C NMR (75 MHz, CDCl₃) δ (ppm) 159.53, 133.56, 133.53, 114.41, 113.96, 83.78, 75.72, 68.00, 31.89, 29.43, 29.32, 29.23, 26.08, 22.73, 14.15.

Data for 2-ethynyl-6-heptyloxynaphthalene (**7c**). Yield 83%; white solid; ¹H NMR (300 MHz, CDCl₃) δ (ppm) 7.94 (s, 1H, Ar-H), 7.67 (m, 2H, Ar-H), 7.47 (m, 1H, Ar-H), 7.15 (dd, *J* 9.0 Hz, *J* 2.5 Hz, 1H, Ar-H), 7.05 (d, *J* 2.6 Hz, 1H, Ar-H), 4.05 (t, *J* 7.0 Hz, 2H, CH₂O), 3.10 (s, 1H, CCH), 1.84 (m, 2H, CH₂CH₂O), 1.50-1.30 (m, 8H, (CH₂)₆), 0.89 (t, *J* 6.5 Hz, 3H, CH₃); ¹³C NMR (75 MHz, CDCl₃) δ (ppm) 158.02, 134.48, 132.10, 129.25, 129.08, 128.21, 126.81, 119.83, 116.80, 106.47, 84.33, 76.73, 76.68, 68.08, 31.86, 29.25, 29.16, 26.11, 22.70, 14.18.

*e-mail: aloir.merlo@ufrgs.br, willy_glen@yahoo.com.br

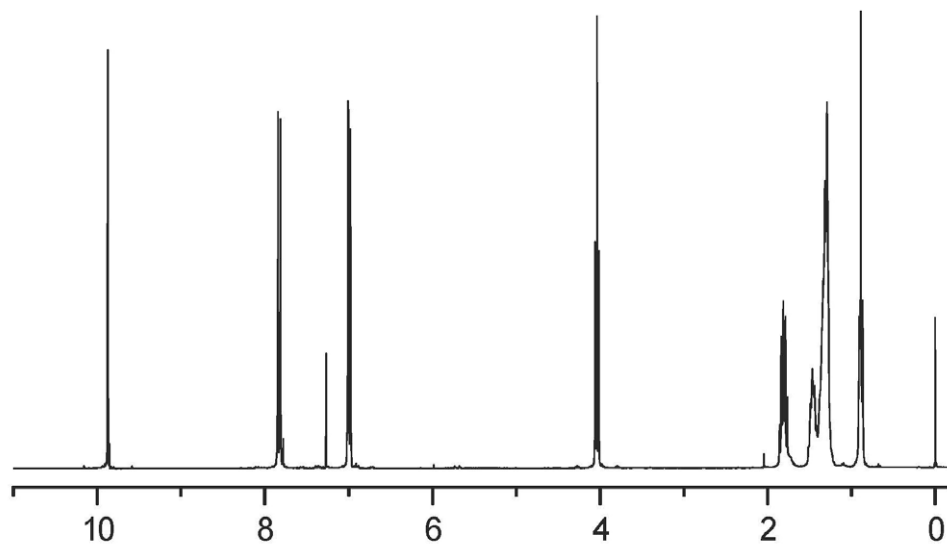


Figure S1. ¹H NMR (300 MHz, CDCl₃) spectrum of compound 2a.

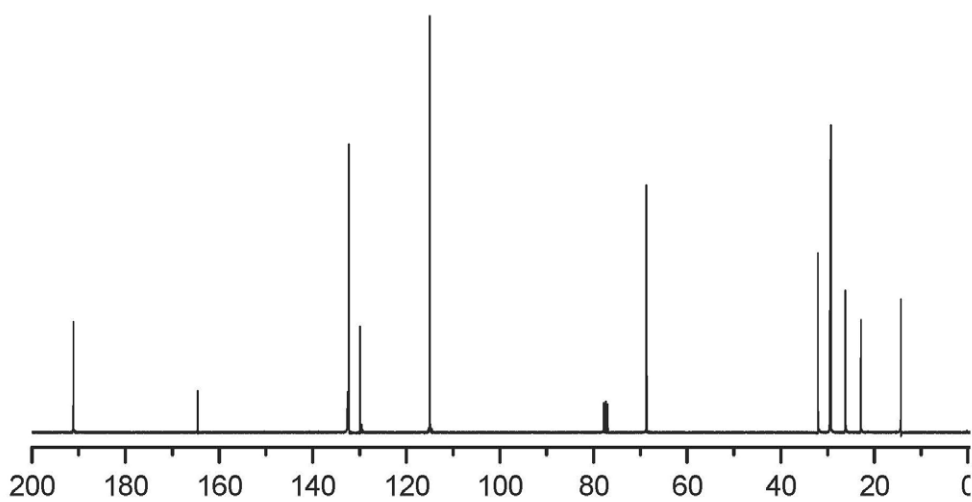


Figure S2. ¹³C NMR (75 MHz, CDCl₃) spectrum of compound 2a.

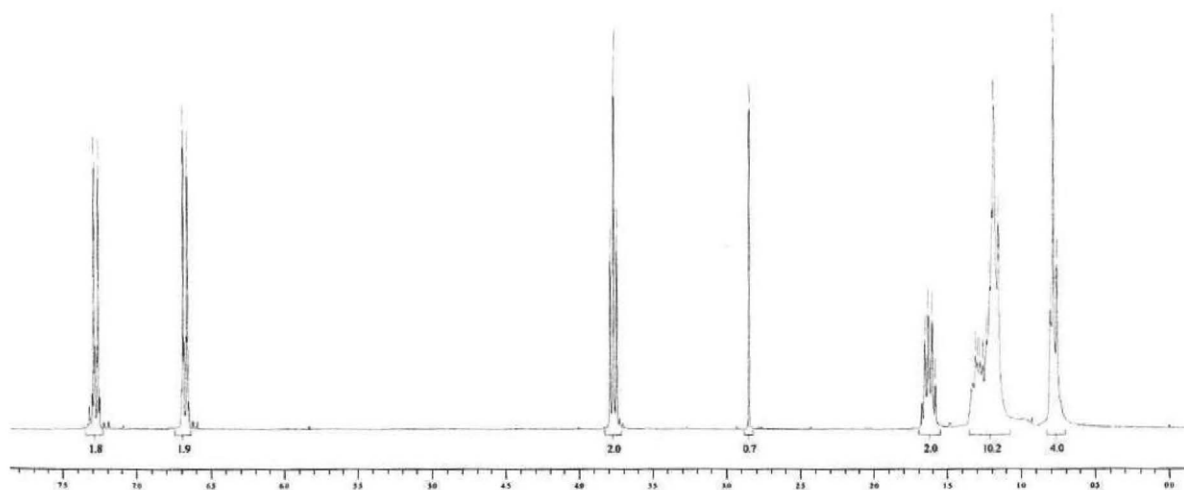


Figure S3. $^1\text{H NMR}$ (300 MHz, CDCl_3) spectra of **7a**.

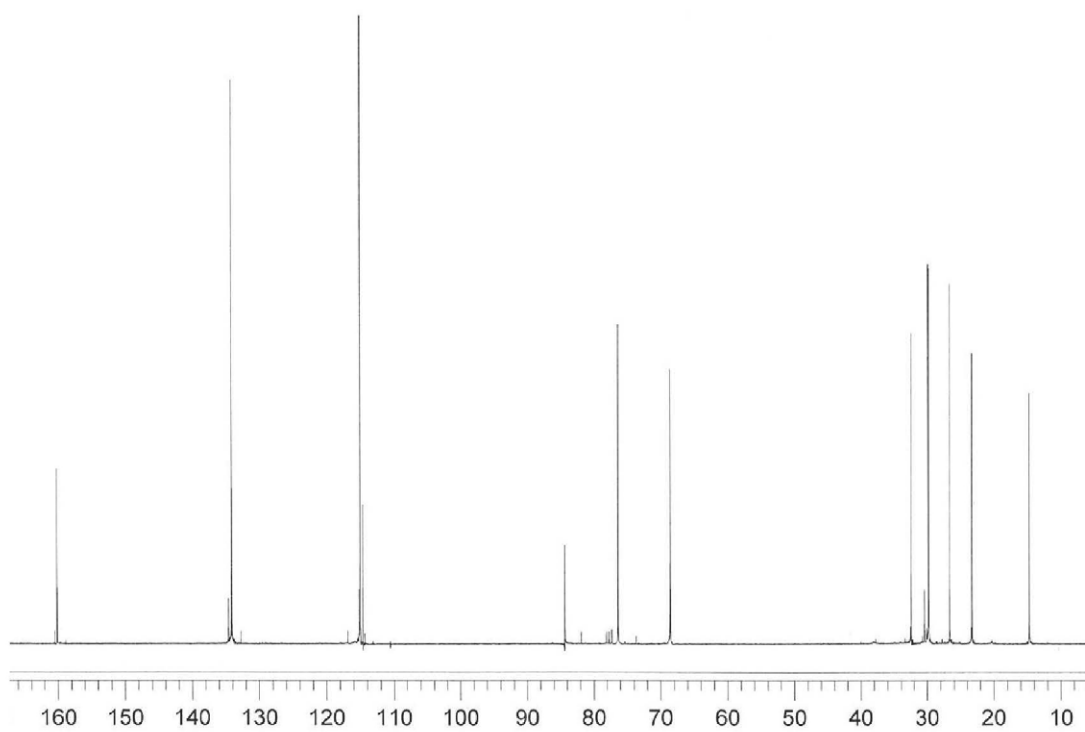


Figure S4. $^{13}\text{C NMR}$ (75 MHz, CDCl_3) spectra of **7a**.

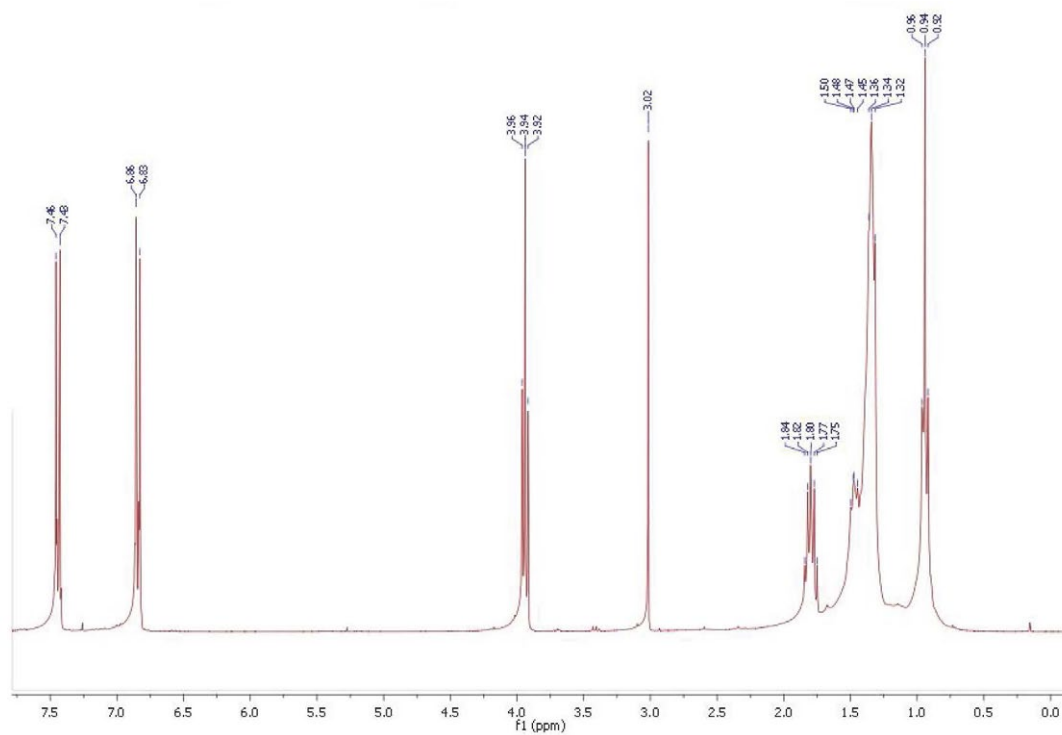


Figure S5. ^1H NMR (300 MHz, CDCl_3) spectra of **7b**.

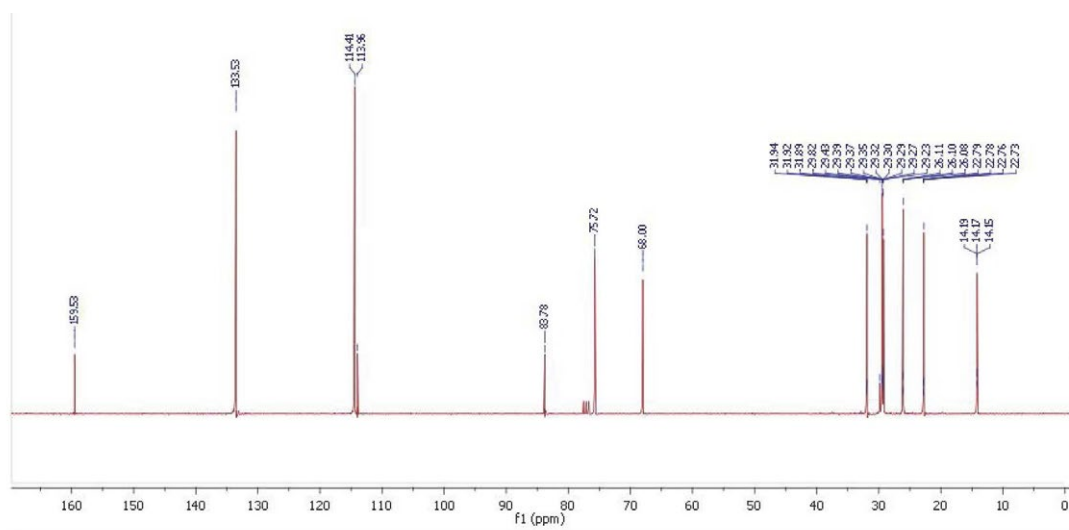


Figure S6. ^{13}C NMR (75 MHz, CDCl_3) spectra of **7b**.

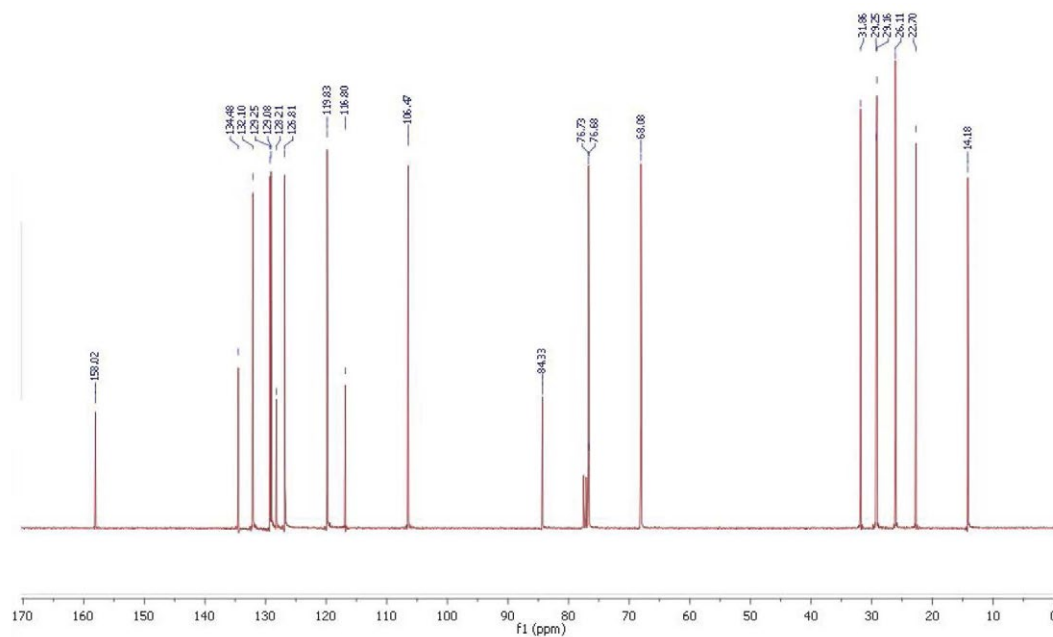


Figure S7. ¹³C NMR (75 MHz, CDCl₃) spectra of 7c.

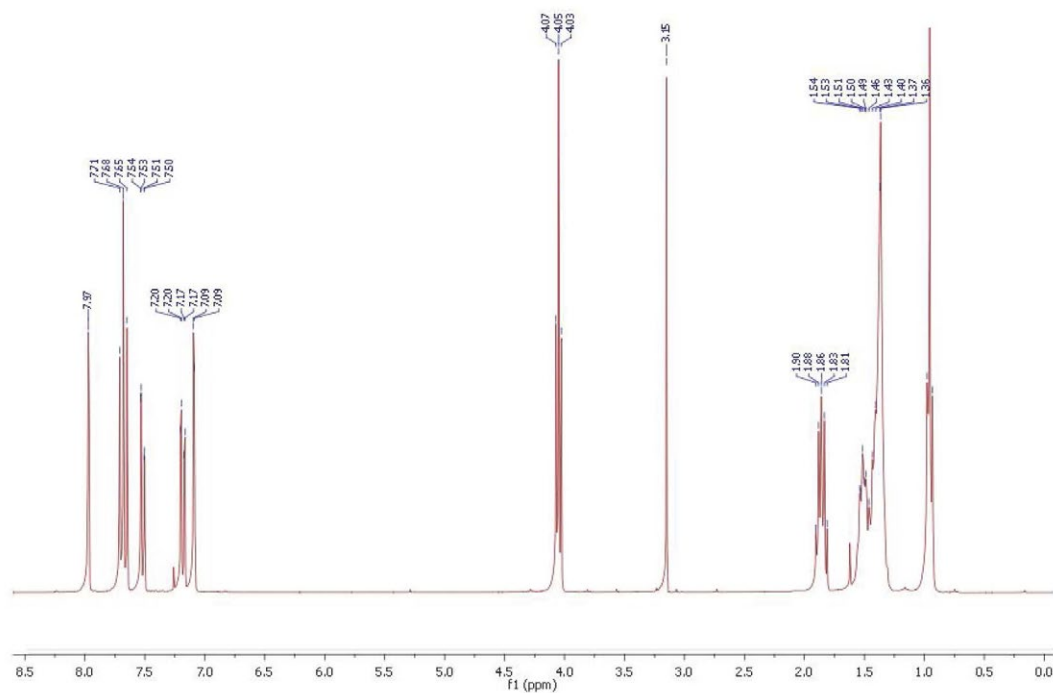


Figure S8. ¹H NMR (300 MHz, CDCl₃) spectra of 7c.

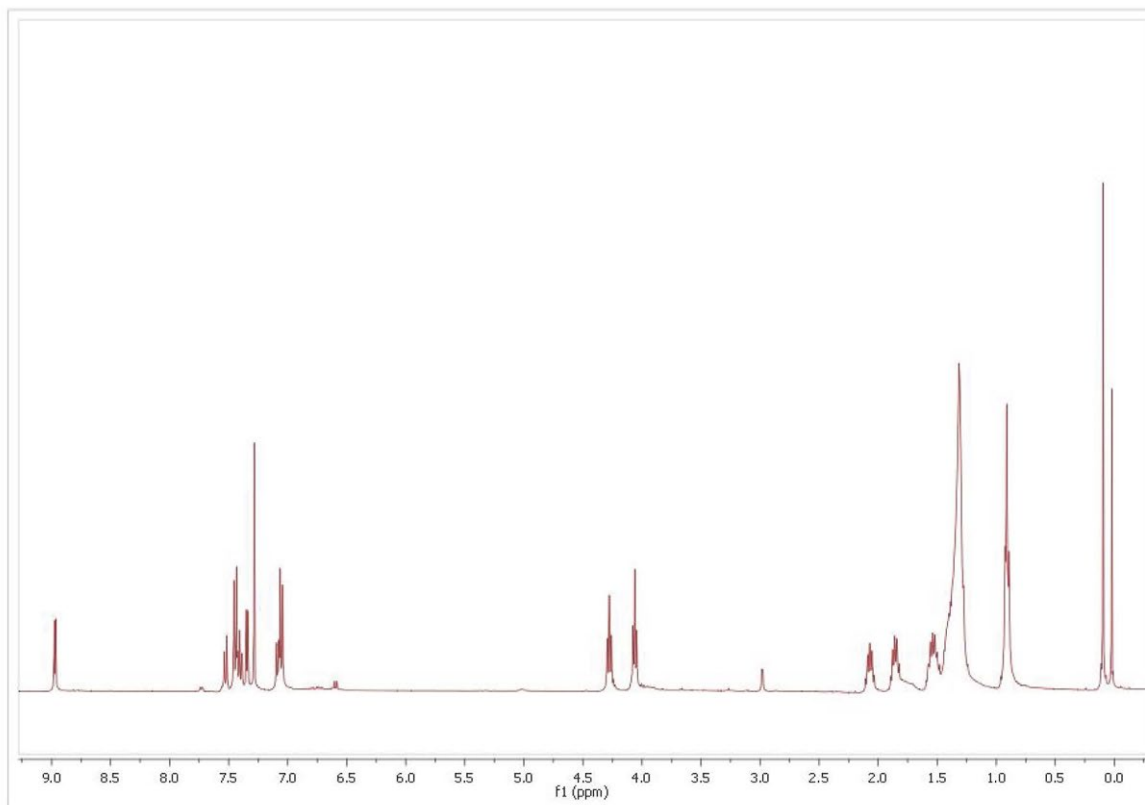


Figure S9. ¹H NMR (300 MHz, CDCl₃) spectra of compound **8a**.

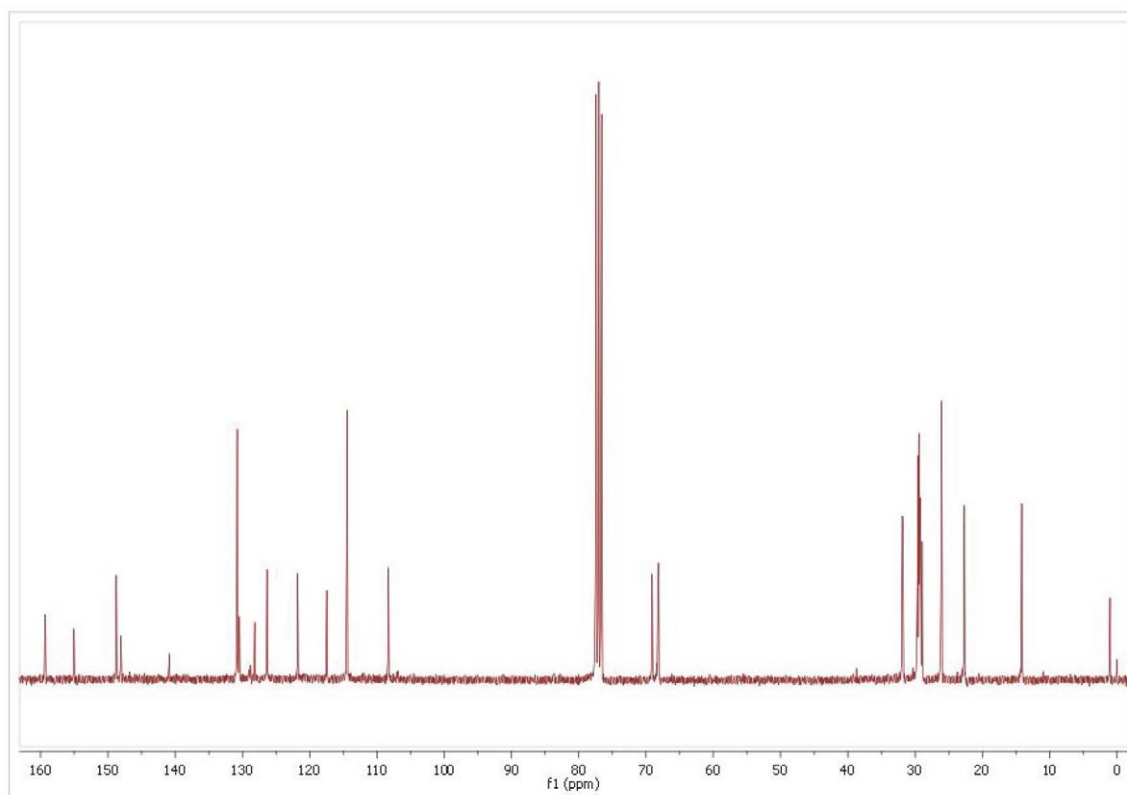


Figure S10. ¹³C NMR (75 MHz, CDCl₃) spectra of compound **8a**.

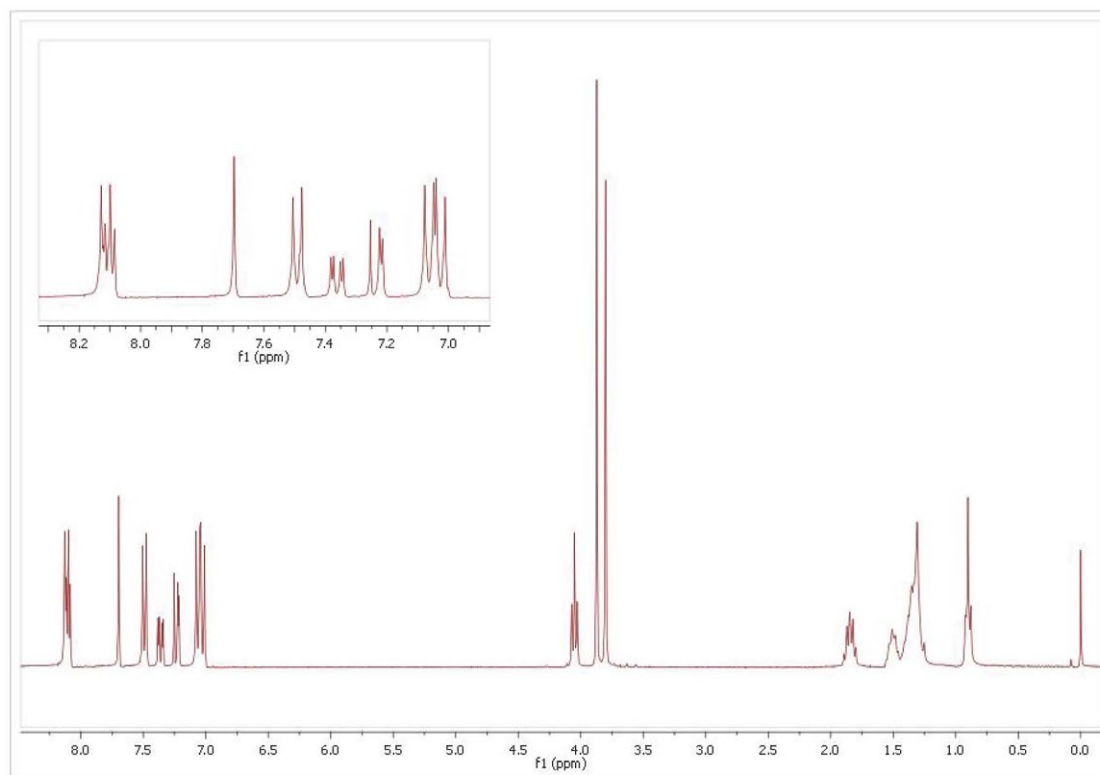


Figure S11. ^1H NMR (300 MHz, CDCl_3) spectra of compound **8b**.

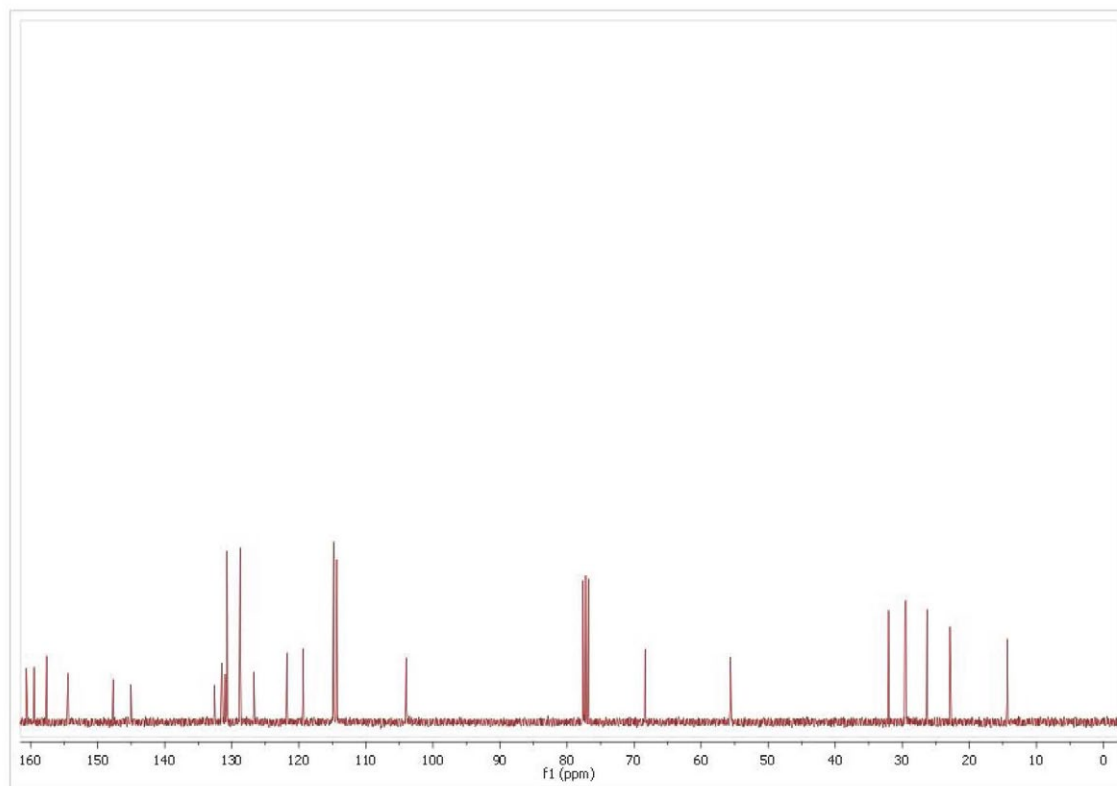


Figure S12. ^{13}C NMR (75 MHz, CDCl_3) spectra of compound **8b**.

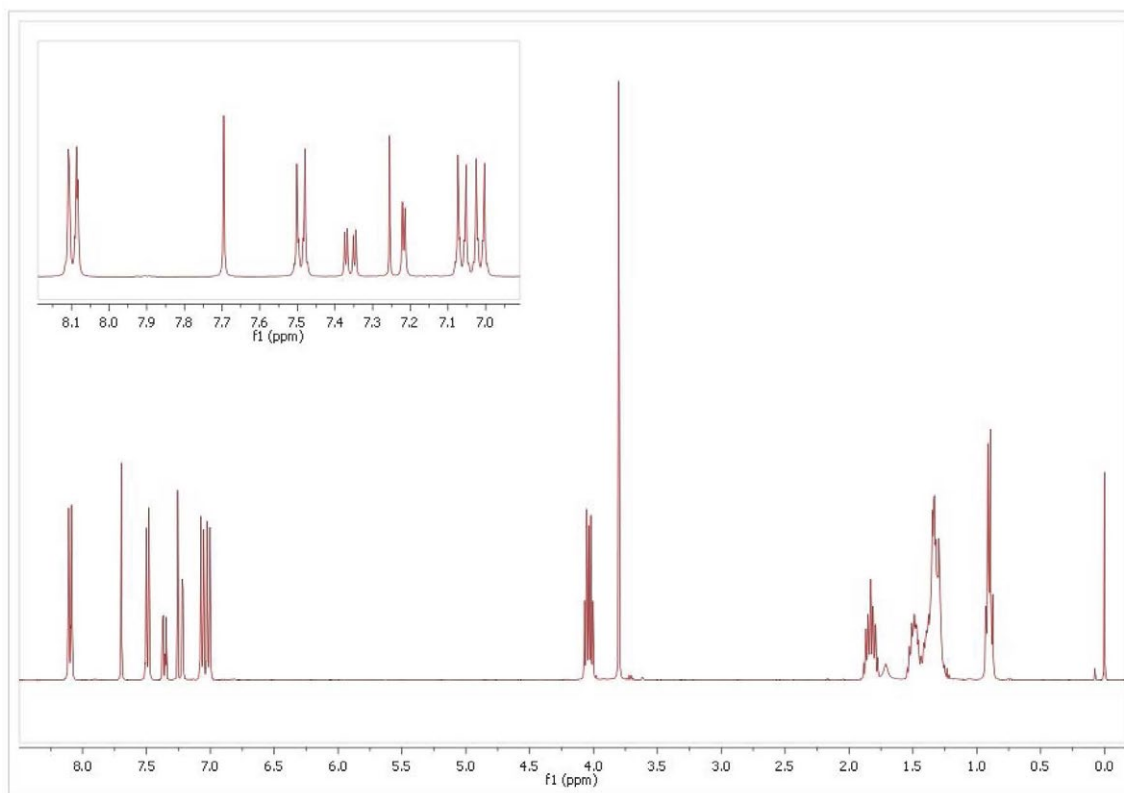


Figure S13. ^1H NMR (300 MHz, CDCl_3) spectra of compound **8c**.

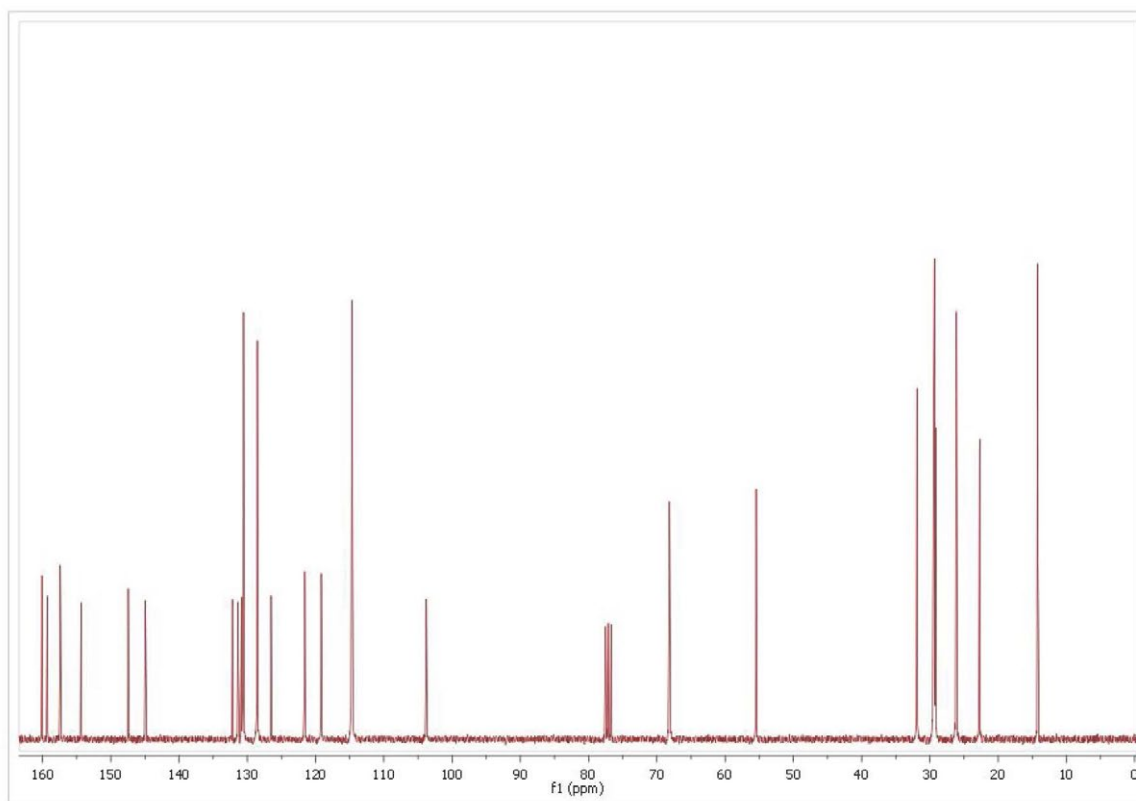


Figure S14. ^{13}C NMR (75 MHz, CDCl_3) spectra of compound **8c**.

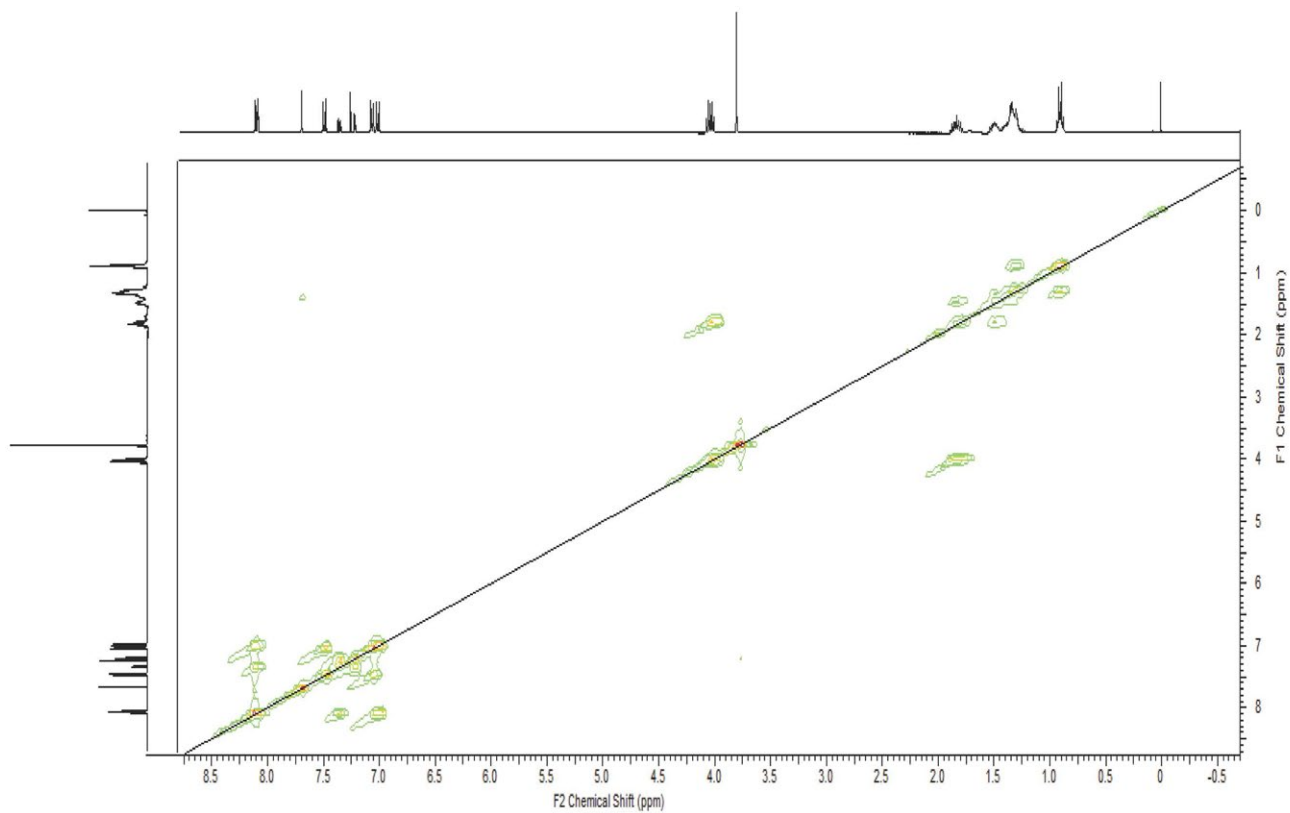


Figure S15. COSY (CDCl₃) spectra of compound **8c**.

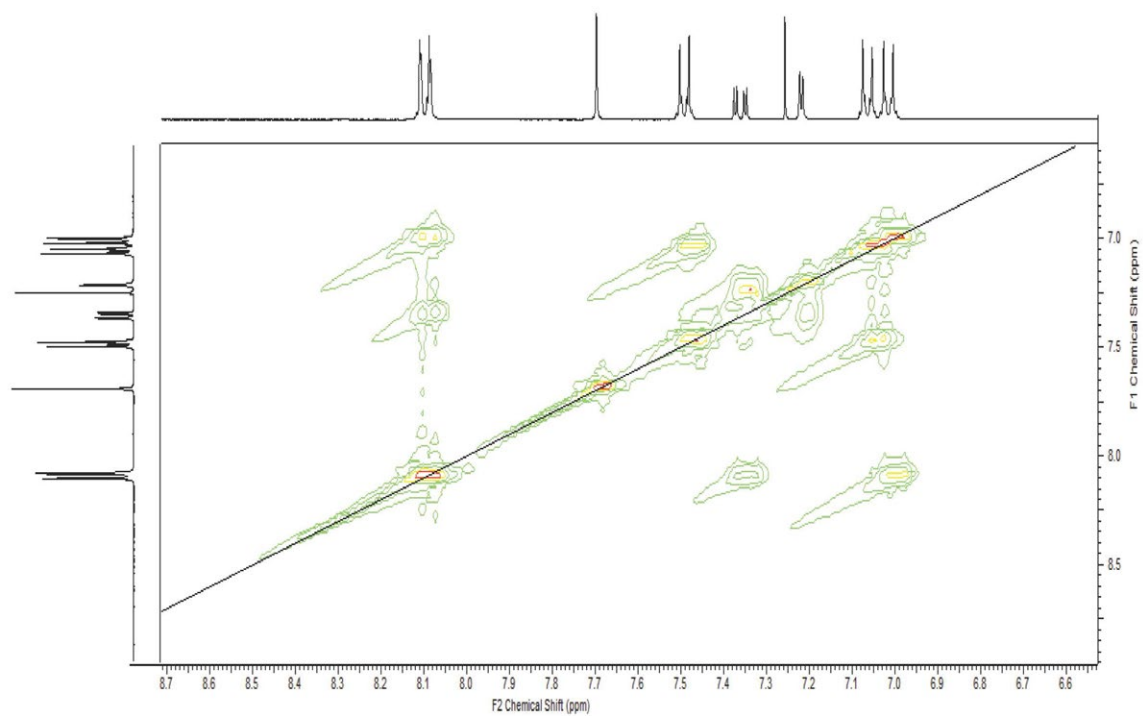


Figure S16. COSY (CDCl₃) spectra of compound **8c**. Aromatic region expansion.

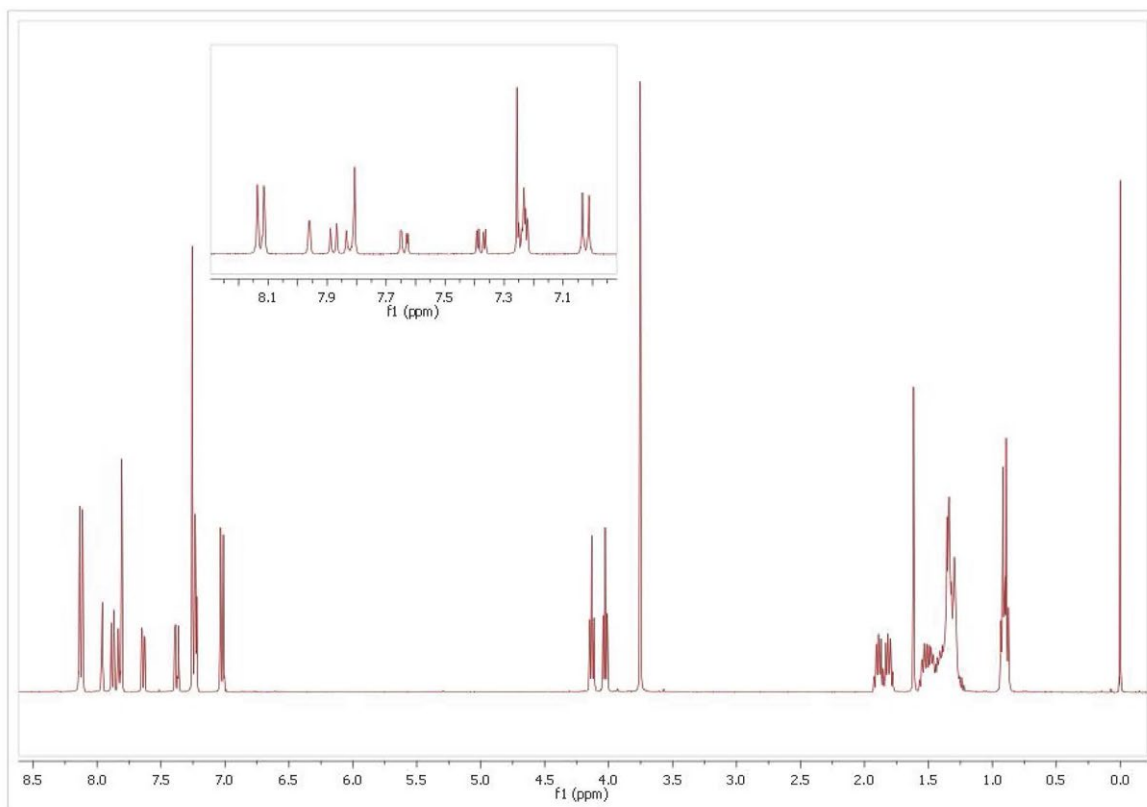


Figure S17. ^1H NMR (300 MHz, CDCl_3) spectra of compound **8d** (1.62ppm- H_2O peak).

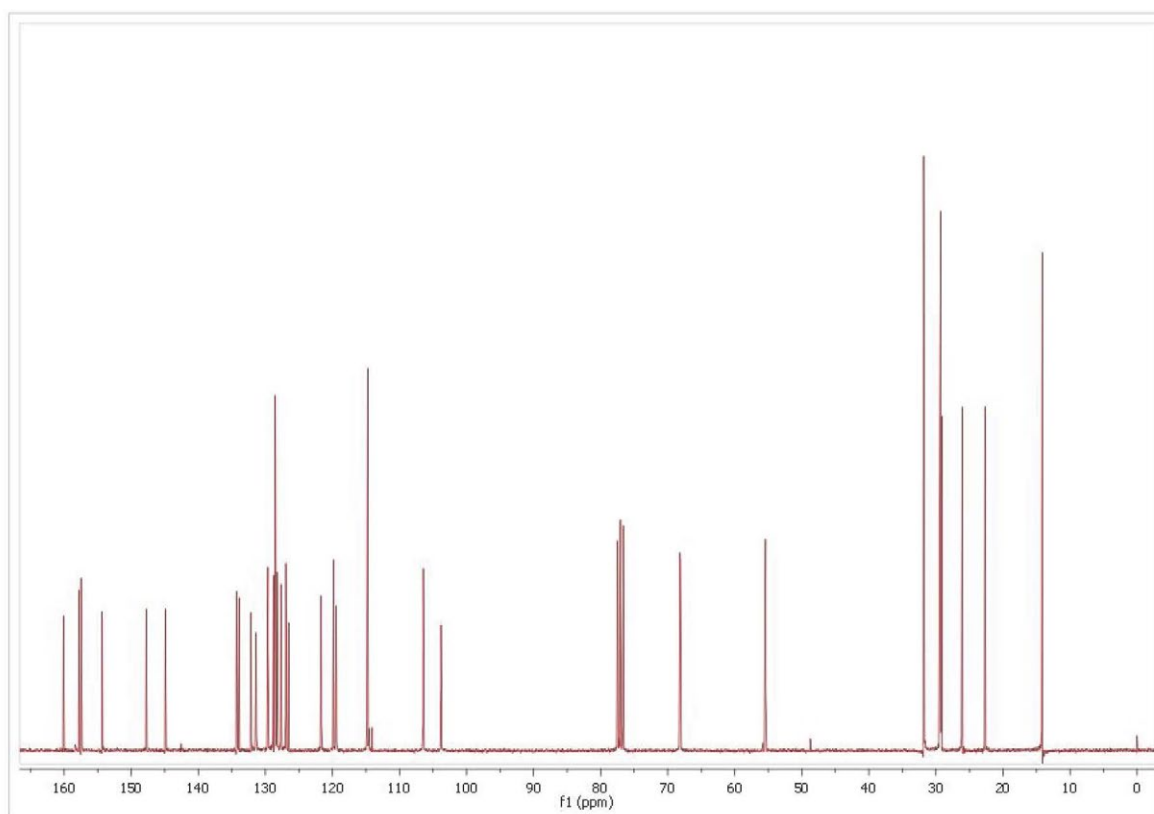


Figure S18. ^{13}C NMR (75 MHz, CDCl_3) spectra of compound **8d**.

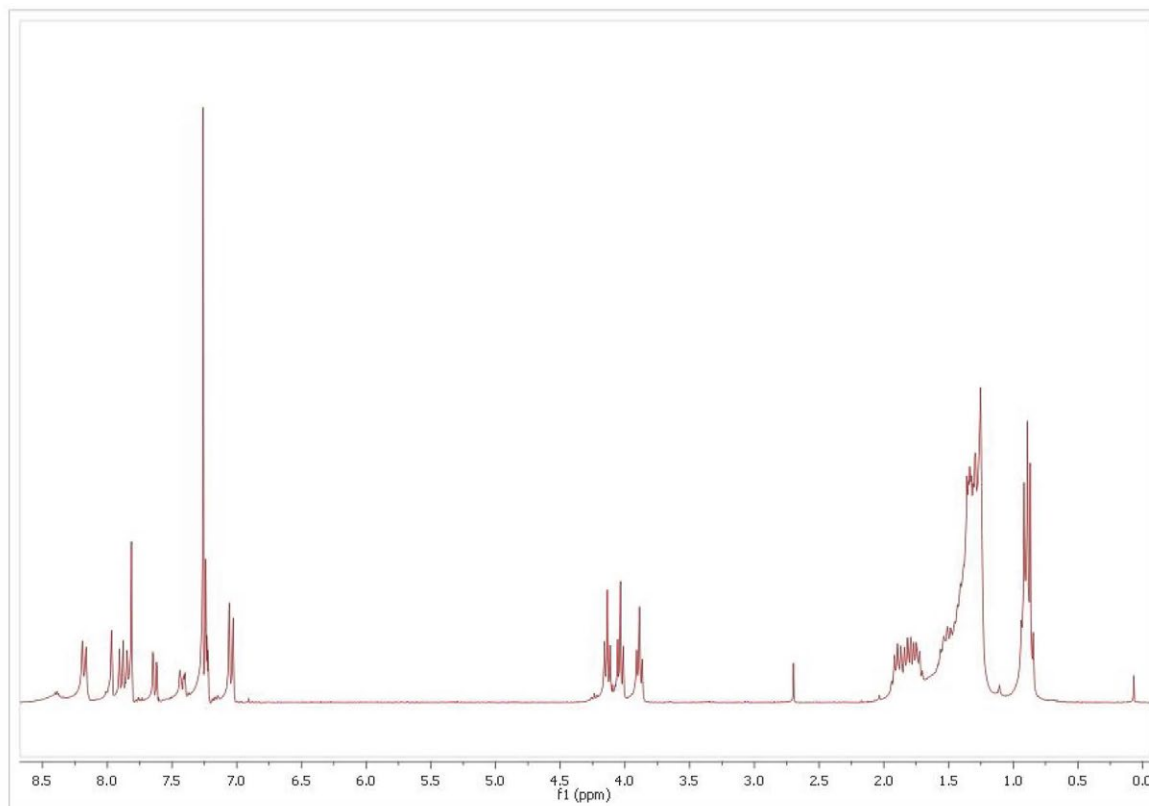


Figure S19. ¹H NMR (300 MHz, CDCl₃) spectra of compound **8e** (2.70 ppm, solvent peak).

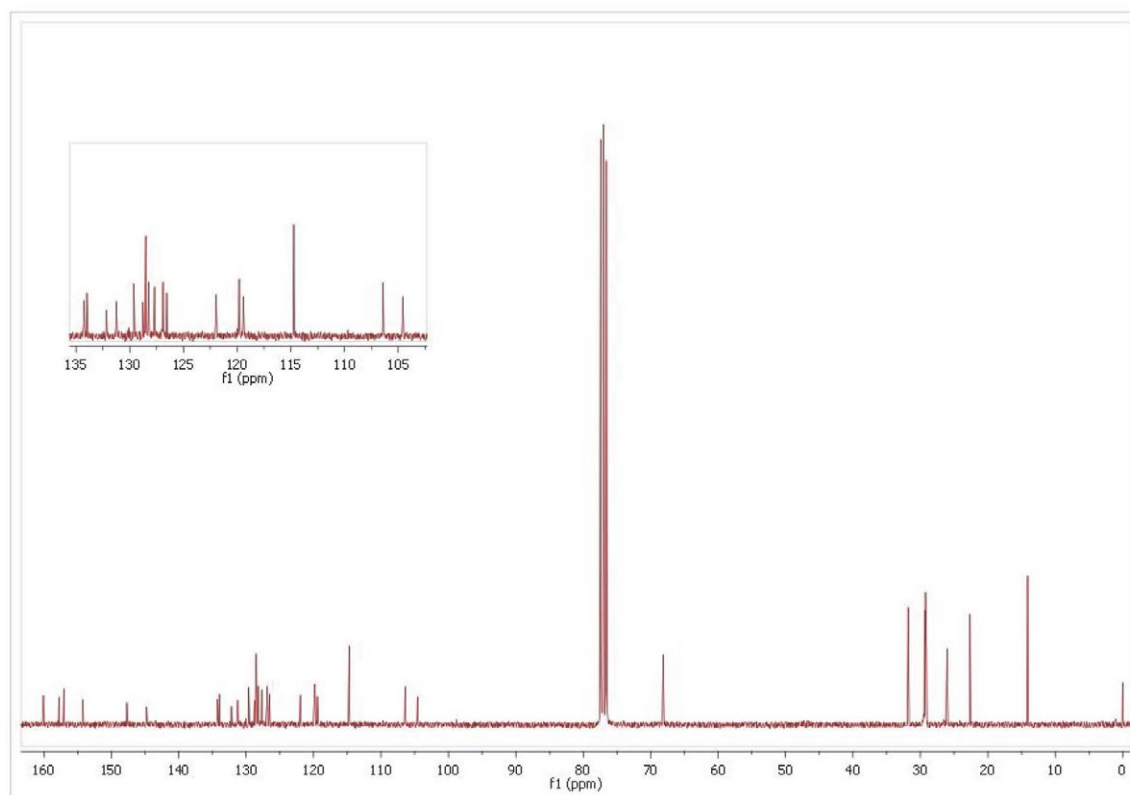


Figure S20. ¹³C NMR (75 MHz, CDCl₃) spectra of compound **8e**.

Electrochemical studies

For estimation of the HOMO and LUMO, **8c** was selected and cyclic voltammetry experiments were carried out in Autolab PGSTAST, using a three compartment cell with a platinum sheet as working electrode, Ag/AgCl electrode as reference and a Pt wire as counter electrode. The quinoline was measured using 0.1 mol L⁻¹ TBAPF₆ in acetonitrile, as supporting electrolyte, at scan rate of 20 mV s⁻¹. The half-wave potential ($E^{1/2}$) of Fc/Fc⁺ measured in 0.1 mol L⁻¹ TBAPF acetonitrile solution is 0.41 V vs. Ag/AgCl.

Cyclic voltammetry results of quinoline **8c** were compared with UV-Vis data. Figure S1 shows the voltammetry curve in 0.1 mol L⁻¹ of TBAPF₆. Figure S1 shows the oxidation and reduction peaks with values of 1.65 V and -0.55 V, respectively. The HOMO and LUMO energy levels were calculated using the oxidation and reduction values in equation 1.

$$E^{\text{HOMO/LUMO}} = [-e(E_{\text{onset (vs. Ag/AgCl)}}) - E_{\text{onset (Fc/Fc}^+ \text{ vs. Ag/AgCl)}}] - 4.8 \text{ eV} \quad (1)$$

Ferrocene potential at -4.8 eV was included to define the zero point. The HOMO energy was calculated as 6.06 (-eV) and the LUMO was 3.76 (-eV), therefore the energy gap from the electrochemical measurements were calculated as $E_{\text{gap}} = 2.3 \text{ eV}$, which is in agreement with the E_{gap} obtained from the optical measurements as describe in the UV-Vis section. The band gap from UV-Vis spectra (1.98 eV) was obtained by extrapolation, using the equation $E_{\text{gap}} = 1240/\lambda \text{ (nm)}$.

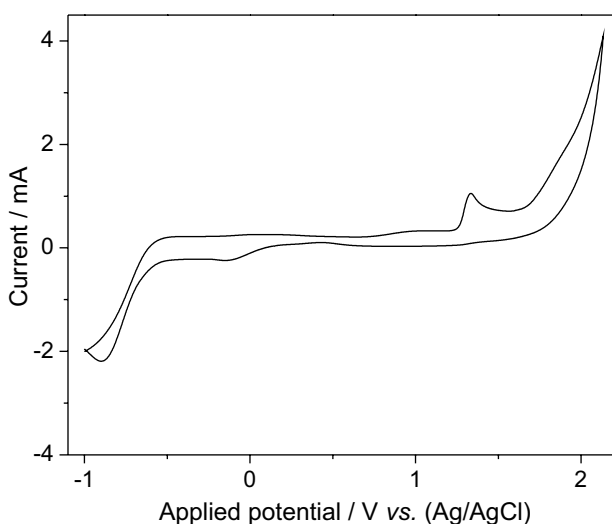


Figure S21. Cyclic voltammogram of the quinoline **8c** in 0.1 mol L⁻¹ of TBAPF₆.

Spectral measurements

Absorption spectra were taken in a Thermo-scientific spectrometer using a 1 cm quartz cuvette. Steady-state fluorescence measurements were made in a HITACHI model F4500 spectrometer. Time-resolved fluorescence of the compounds were measured by time-correlated single-photon counting using a homemade picosecond spectrometer equipped with Glan-Laser polarizers (Newport), a Peltier-cooled PMTMCP (Hamamatsu R3809U-50) as the photon detector, and Tennelec-Oxford counting electronics. The light pulse was provided by frequency doubling the 200 fs laser pulse of a Mira 900 Ti-Sapphire laser pumped by a Verdi 5 W coherent laser, and the pulse frequency was reduced to 800 kHz using a Conoptics pulse picker. The fluorescence decays were excited at 400 nm and decay results were analyzed by a reconvolution procedure with instrument response function (irf). Fluorescence decay times were fitted with a bi-exponential function, optimizing Chi square, residuals, and standard deviation parameters. All solutions were deaerated by bubbling oxygen-free nitrogen. The mean fluorescence decay was calculated according to equation 2:

$$\langle \tau \rangle = \frac{A_1 \tau_1 + A_2 \tau_2}{100} \quad (2)$$

where the τ_i is the individual decay time and A_i are the corresponding relative amplitudes. For fluorescence quantum yield experiments, the solutions were placed in 1 cm quartz cuvette and the absorbance of the compounds solutions was set at 0.1-0.2 to minimize inner-filter effects and the presence of aggregates. Transient absorption spectra were obtained using a LFP-112 Luzchem nanosecond laser flash photolysis spectrometer. Excitation of the samples was performed with the third harmonic (355 nm) of a Brio Nd-YAG laser, with 5.2 ns pulses. Kinetic analyses were made with the Luzchem proprietary software.

The fluorescence quantum yield at 293 K was obtained by comparison with the emission of anthracene in ethanol ($\Phi_f = 0.27$).¹ The quantum yields were calculated according to equation 3:

$$\Phi_f = \frac{\int I(\lambda) d\lambda}{\int I(\lambda)^o d\lambda} \times \frac{DO_o}{DO} \times \frac{n^2}{n_o^2} \times \Phi_f^o \quad (3)$$

where the subscript "o" indicates the reference solution, DO is the optical density, Φ_f is the fluorescence quantum yield, $\int I(\lambda)$ is the integrated fluorescence intensity, and n is the refractive index of the solvent. The quantum yield at 77 K was calculated using equation 4:²

$$\Phi_F^{77K} = \frac{\int^{77K} I(\lambda) d\lambda}{\int^{293K} I(\lambda)^0 d\lambda} \times \Phi_F^{293K} \times f_c \quad (4)$$

where f_c is the solvent contraction constant (0.84) at 77 K, and $\int^{77K} I(\lambda) d\lambda$ and $\int^{293K} I(\lambda)^0 d\lambda$ are the areas of the fluorescence emission at 77 K and 293 K, respectively.

Ground-state and excited singlet-state

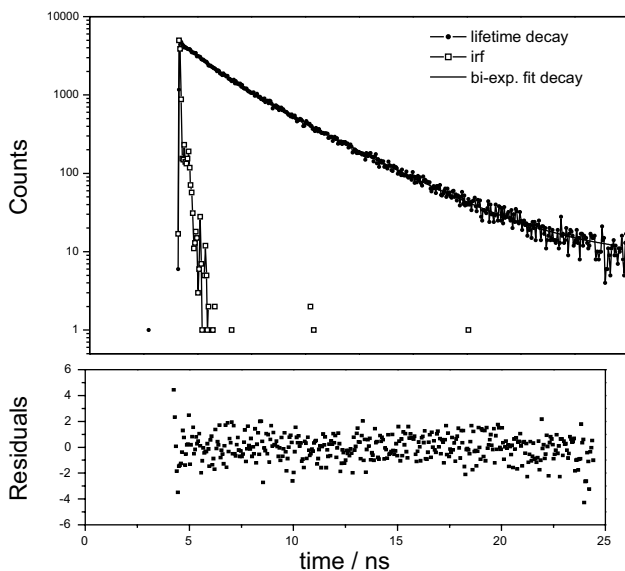


Figure S22. Fluorescence decay and residuals of quinoline **8d** following a bi-exponential fit decay. $\lambda_{exc} = 400$ nm and $\lambda_{em} = 420$ nm.

Exponential components analysis (reconvolution for fluorescence decay)

Fitting range: [87; 500] channels

χ^2 : 1.066

decay	B_i	ΔB_i	$f_i / \%$	$\Delta f_i / \%$	t_i / ns	$\Delta t_i / ns$
1	0.2725	0.0313	25.464	3.882	1.174	0.044
2	0.3128	0.0157	74.536	3.866	2.994	0.005

Table S1. Solvent effect on the photophysical properties of **8e**

Solvent	λ_{MAX}^{abs} / nm		λ_{MAX}^{ems} / nm	λ_{ST} / nm	$\epsilon / (L mol^{-1} cm)$	
	$\pi-\pi^*$	$n-\pi^*$			$\pi-\pi^*$	$n-\pi^*$
Acetonitrile	288	350	400	50	5.9×10^4	1.5×10^4
Ethanol	287	350	400	50	8.3×10^4	2.5×10^4
Cyclohexane	285	350	389	39	6.0×10^4	1.3×10^4

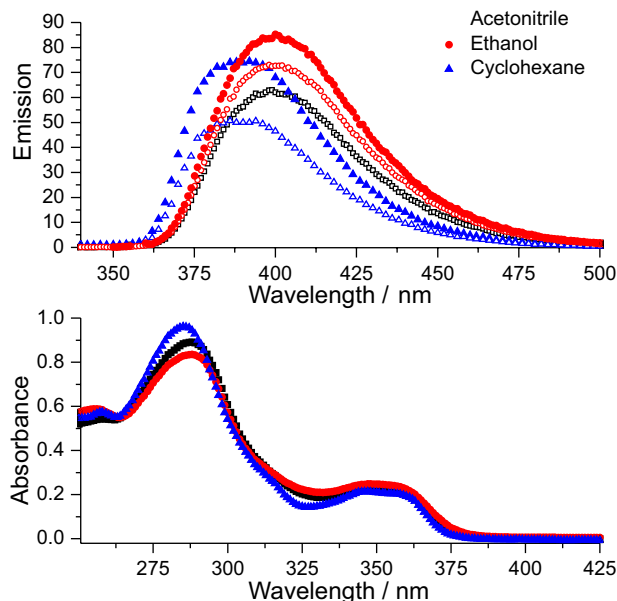


Figure S23. Absorption and emission spectra recorded to the quinoline **8b** in acetonitrile (■ black), ethanol (● red) and cyclohexane (▲ blue).

Crystallographic analysis

Crystallographic analysis was carried out with a single crystal Bruker APEX II DUO diffractometer using graphite-monochromated MoK α radiation (0.71073 Å) from a sealed tube operating at 1.5 kW and the temperature was set at 173 (± 2) K with an Oxford Instruments Cryojet system. Measurements were recorded by phi and omega scans with exposures of 30 s by frame using APEX2.³ All collected data were corrected for Lorentz and polarization effects.⁴ Due to very small absorption coefficient, no absorption correction was applied to the intensities. The structure was solved by direct methods and refined applying the full-matrix least-squares method using SIR97⁵ and SHELXL97⁶ software programs, respectively. All non-hydrogen atoms were refined with anisotropic displacement parameters. Hydrogen atoms were placed at their idealized positions with distances of 0.93 Å for C-H_{Air}, 0.97 Å for C-H₂ and 0.96 Å for C-H₃ groups. The U_{iso} values for the hydrogen atoms were fixed at 1.2 times (for aromatic compounds and methylene) and 1.5 times (for methyl) the U_{eq} of the carrier atom (C). ORTEP plot of the molecular structure

was produced with the PLATON program.⁷ Further crystallographic information are shown in Table S2. Full tables containing the crystallographic data (except structure factors) have been deposited at the Cambridge Structural Database (CCDC 982481) and these data are available free of charge at www.ccdc.cam.ac.uk.

Table S2. Crystal data and structure refinement for **8e**

Empirical formula	C ₄₉ H ₆₅ NO ₃
Formula weight	716.02
Temperature	173(2) K
Wavelength	0.71073 Å
Crystal system	Triclinic
Space group	Pī
Unit cell dimensions	a = 9.5071(3) Å b = 12.4764(4) Å c = 18.5693(6) Å α = 74.758(2)° β = 77.999(2)° γ = 84.217(2)°
Volume	2076.18(11) Å ³
Z	2
Density (calculated)	1.145 mg m ⁻³
Absorption coefficient	0.069 mm ⁻¹
F(000)	780
Crystal size	0.40 × 0.20 × 0.04 mm ³
Theta range for data collection	1.69 to 28.00°
Index ranges	-12 ≤ h ≤ 11, -16 ≤ k ≤ 16, -24 ≤ l ≤ 24
Reflections collected	26902
Independent reflections	10036 (R _{int} = 0.0179)
Refinement method	Full-matrix least-squares on F ²
Data/restraints/parameters	10036/0/481
Goodness-of-fit on F ²	1.043
Final R indices [I > 2σ(I)]	R1 = 0.0483, wR2 = 0.1351
R indices (all data)	R1 = 0.0623, wR2 = 0.1471
Largest diff. peak and hole	0.388 and -0.223 e Å ⁻³

References

- Berlman, I. B.; *Handbook of Fluorescence Spectra of Aromatic Molecules*, Academic Press: New York, 1971; Dawson, W. R.; Windsor, M. W.; *J. Phys. Chem.* **1968**, *72*, 3251.
- Biczók, L.; Bérces, T.; Linschitz, H.; *J. Am. Chem. Soc.* **1997**, *119*, 11071; Leigh, W. J.; Lathioor, E. C.; Pierre, M. J. S.; *J. Am. Chem. Soc.* **1996**, *118*, 12339.
- APEX II, Data Collection Software*, version 2011.8-0; Bruker AXS Inc.: Madison, WI, 2005-2011.
- Bruker APEX2, SAINT, Bruker AXS Inc., Madison, Wisconsin, USA, 2009.
- Altomare, A.; Burla, M. C.; Camalli, M.; Cascarano, G. L.; Giacovazzo, C.; Guagliardi, A.; Moliterni, A. G. G.; Polidori, G.; Spagna, R.; *J. Appl. Crystallogr.* **1999**, *32*, 115.
- Sheldrick, G. M.; *Acta Crystallogr.* **2008**, *A64*, 112.
- Spek, A. L.; *J. Appl. Crystallogr.* **2003**, *36*, 7; Bruno, I. J.; Cole, J. C.; Edgington, P. R.; Kessler, M. K.; Macrae, C. F.; McCabe, P.; Pearson, J.; Taylor, R.; *Acta Crystallogr.* **2002**, *B58*, 389.